

# Investigation of the factors determining the SIMS depth resolution in silicon-isotope multiple layers

M. Tomita,<sup>a)</sup> M. Koike, H. Akutsu, and S. Takeno

Corporate Research and Development Center, Toshiba Corporation, 8 Shinsugita-cho, Isogo-ku, Yokohama 235-8522, Japan

Y. Kawamura, Y. Shimizu,<sup>b)</sup> M. Uematsu, and K. M. Itoh

School of Fundamental Science and Technology, Keio University, 3-14-1 Hiyoshi, Kohoku-ku, Yokohama 223-8522, Japan

(Received 29 August 2011; accepted 28 October 2011; published 13 December 2011)

In order to identify their controlling factors, the depth resolution parameters for secondary ion mass spectrometry, which include the decay length and the standard deviation of the Gaussian function (also referred to as the depth resolution function), for silicon atoms in a silicon matrix with silicon-isotope multiple layers were investigated under oxygen ( $O_2^+$ ) and cesium ( $Cs^+$ ) ion bombardments with a wide ion energy range (from 200 eV to 10 keV) and with several incident angles. The use of silicon-isotope multiple layers in this investigation eliminated the chemical segregation effect caused by the sample composition. Measures were also taken to prevent ripple formation on the sputtered sample surface. The obtained depth resolution parameters were proportional to  $E^{1/2}\cos\theta$ , where  $E$  is the primary ion energy per atom and  $\theta$  is the incident angle relative to the surface normal. The relationships for decay length and standard deviation were different for the  $Cs^+$  ion, the  $O_2^+$  ion with full oxidization, and the  $O_2^+$  ion without full oxidization. The damage depth was measured by high-resolution Rutherford backscattering spectrometry and it was found that the relationships of the standard deviation versus damage depth depend only on the damage depth with a small dependence on the ion species ( $O_2^+/Cs^+$ ). The degree of mixing near the sputtered surface of thin silicon-isotope multiple layers bombarded by  $O_2^+/Cs^+$  ions was measured using laser-assisted atom probe analysis, and the relationship of the degree of mixing with the depth resolution parameters indicated that the decay length was degraded according to the degree of mixing. Atomic mixing/sputtering simulations revealed the factors determining the depth resolution parameters for secondary ion mass spectrometry. The standard deviation is found to be mainly degraded by the damage depth, which agrees with the results obtained by Rutherford backscattering spectrometry, whereas the decay length is mainly extended by the variance of the damage density profile, which is a parameter of the Gaussian function and governs the degree of mixing near the surface. © 2012 American Vacuum Society. [DOI: 10.1116/1.3669400]

## I. INTRODUCTION

Improvement of depth resolution in secondary ion mass spectrometry (SIMS) analysis is a critical issue for depth profiling of silicon semiconductor films because the film thickness and the depth of an implanted dopant have been reduced to the level of a few nanometers. For example, the gate oxide thickness should be less than  $\sim 5$  nm and the depth of implanted dopant in shallow junctions should be less than  $\sim 10$  nm.<sup>1</sup>

Substantial efforts have been made to understand the effects of ion bombardment on SIMS depth resolution in order to improve it. Dowsett *et al.* proposed a SIMS depth resolution function (response function for SIMS analysis),<sup>2</sup> and Chu and Dowsett later showed that the depth resolution function is a convolution of two functions, namely, the exponential decay function and the Gaussian function, with two parameters.<sup>3</sup> The first parameter is the decay length,  $\lambda_d$ , which represents the length over which the signal of the

SIMS depth resolution function attenuates exponentially to  $1/e$ , whereas the second parameter is the standard deviation,  $\sigma$ , of the Gaussian function, which represents the blurring of the SIMS depth resolution function in both the depth and surface directions. Note that exponential decay always overshadows Gaussian blurring in the depth direction, but Gaussian blurring is evident in the surface direction. The major effects of ion bombardment on the SIMS depth resolution include atomic (cascade) mixing, chemical segregation, and surface roughening including ripple formation. In some cases, primary recoil mixing, radiation enhanced diffusion, and preferential sputtering may also be significant as described in some studies, e.g., Linnarsson and Svensson.<sup>4</sup> Ripple formation by bombardment of oxygen ( $O_2^+$ ) and cesium ( $Cs^+$ ) ions, which are usually used in SIMS depth profiling, can be suppressed under the reported bombardment conditions.<sup>5-8</sup> Separation of the atomic mixing effect and the chemical segregation effect is, however, difficult in general. The mechanism for degradation of the depth resolution by ion bombardment, which is a combination of the contributions of atomic mixing and chemical segregation to the depth resolution, is unclear.

<sup>a)</sup>Electronic mail: mitsuhiro.tomita@toshiba.co.jp

<sup>b)</sup>Present address: The Oarai Center, Institute for Materials Research, Tohoku University, 2145-2 Narita, Oarai, Ibaraki 311-1313, Japan.

It is possible to evaluate the atomic mixing effect without the chemical segregation effect by using isotope multiple layers. Wittmaack and Poker studied the depth resolution parameters by bombarding thick silicon isotope multiple layers (thickness: 30–100 nm, ion beam deposition) with various ions [ions of several different noble gas elements, cesium, oxygen ( $O_2^+$ ), and nitrogen ( $N_2^+$ )] at near normal incidence (within  $2^\circ$  from the surface normal) with an energy of more than 2 keV.<sup>9</sup> They found that the decay length measured by bombardment of noble gas ions and cesium ions was governed by the ion energy per atom and not by the penetration depth (primary ion mass). They also found that the width of the leading edge parameter of the depth resolution function (width of between 1% and 50% of the plateau intensity) depended on the primary ion mass.

Linnarsson and Svensson have reported decay lengths measured by the bombardment of AlGaAs/GaAs multiple layers with several different noble gas ions,<sup>4</sup> and their results agree with those of Wittmaack and Poker.<sup>9</sup> They have also found the decay lengths to be proportional to  $E^{1/2}\cos\theta$ , where  $E$  is the energy of the primary ion and  $\theta$  is the angle of incidence of the primary ion relative to the surface normal. This relationship is fully consistent with the diffusion model for atomic mixing.

In the case of  $O_2^+$  or  $N_2^+$  ions with near normal incidence in the study by Wittmaack and Poker, surface oxidation or nitridation of the silicon surface buffers the atomic mixing.<sup>9</sup> Also, the decay lengths for  $O_2^+$  and  $N_2^+$  ion bombardments were shorter than those for noble gas and cesium ion bombardments.  $O_2^+$  ion bombardment enhances the positive secondary ion yield and is usually used in SIMS analysis with both normal (or near-normal) incidence, which provides a fully oxidized silicon surface, and oblique (around  $60^\circ$ ) incidence, which provides a silicon surface that is not fully oxidized. It is thought that different surface states (fully oxidized or not fully oxidized) lead to differences in the variation of the SIMS depth resolution parameters (decay length and standard deviation) with the  $O_2^+$  ion energy, but there is no data available for  $O_2^+$  ion bombardment with oblique incidence for silicon isotope multiple layers. Continuous progress in SIMS instrumentation has led to the development of a low-energy ion gun that emits  $O_2^+$  and  $Cs^+$  ion beams with energies of less than 250 eV and; therefore, the behaviors of the SIMS depth resolution parameters, which are governed only by the atomic mixing effect (no chemical segregation effect) under low energy  $O_2^+$  and  $Cs^+$  ion bombardments, can be determined.

In this study, the atomic mixing effects (depth resolution functions) of  $O_2^+$  and  $Cs^+$  ion bombardments with a wide ion energy range (from 200 eV to 10 keV) and several incident angles, resulting in sputtered surfaces that were fully oxidized or not fully oxidized by the  $O_2^+$  ion bombardment, were investigated without the chemical segregation effect by using silicon-isotope multiple layers deposited by molecular beam epitaxy (MBE) with flat surfaces and sharp interfaces between isotope layers. As conditions, reported in several studies,<sup>5–8</sup> that ensured no ripples on the sputtered surface were used, the obtained depth resolution function could be

assumed to be affected only by the atomic mixing effect. The factors determining the SIMS depth resolution function in atomic mixing are therefore discussed based on the following: ion-bombardment damage depths measured using aligned high-resolution Rutherford backscattering spectrometry (aligned HR-RBS), mixing depths and degree of mixing measured using laser-assisted atom probe (AP) analysis, and atomic mixing/sputtering simulations.

The damage depths of silicon surfaces bombarded by  $O_2^+/Cs^+$  ions were evaluated using aligned HR-RBS. The damage depth measured using aligned HR-RBS corresponds to the short-range displacement of silicon atoms from the periodic position in the silicon crystal during atomic mixing (cascade mixing). The mixing depth and the degree of mixing near the sputtered surface resulting from the ion bombardment were measured for thin silicon-isotope multiple layers (thickness of each layer:  $\sim 2.6$  nm) using AP analysis. The measurements were performed referring to studies on the displacement of silicon atoms by B/As ion implantation into silicon isotope superlattices.<sup>10,11</sup> In this study, the terms “mixing depth” and “damage depth” by ion bombardment are not used interchangeably. The mixing depth obtained by AP analysis of thin silicon-isotope multiple layers is a measure of the long-range atomic mixing by the exchange of silicon isotope atoms between isotope layers. The degree of mixing refers to the degree of mixing of the atoms of different isotope layers. The use of thin silicon-isotope multiple layers enables direct observation of the atomic mixing of silicon atoms in the depth direction. The atomic mixing/sputtering simulations were performed referring to the work of Linnarsson and Svensson, which was based on a diffusion model for atomic mixing.<sup>4</sup> From the results of the simulations, the factors determining the SIMS depth resolution parameters were identified.

## II. EXPERIMENT

The  $^{28}\text{Si}/^{30}\text{Si}$  isotope multiple layer samples were prepared on Si (001) substrates by MBE. These isotope layers were grown at  $650^\circ\text{C}$ , with growth rates of  $1.2 \times 10^{-3}$  nm/s for  $^{28}\text{Si}$  layers and  $2.1 \times 10^{-3}$  nm/s for  $^{30}\text{Si}$  layers, by the Itoh group in Keio University.<sup>10,12,13</sup> Of these samples, some (referred to as sample A) were used for SIMS measurements which were performed to evaluate the SIMS depth resolution function, while others (referred to as sample B) were used for AP analysis, which was performed to evaluate the mixing depth and the degree of mixing. The structures of the samples for the SIMS measurements and the AP analysis are shown in Figs. 1(a) and 1(b), respectively. Sample B had 18 sets of  $^{28}\text{Si}$  ( $\sim 2.6$  nm)/ $^{30}\text{Si}$  ( $\sim 2.6$  nm) layers. To evaluate the damage depth of the silicon surface for various  $O_2^+/Cs^+$  ion bombardment conditions, Si (001) substrates bombarded with  $O_2^+$  or  $Cs^+$  ions (referred to as sample C) were examined using aligned HR-RBS.

Before SIMS measurements of sample A, structures including interdiffusion (intermixing) at the  $^{28}\text{Si}/^{30}\text{Si}$  interfaces during the growth were evaluated in detail using AP analysis. Figure 2 shows the silicon isotope depth profiles for

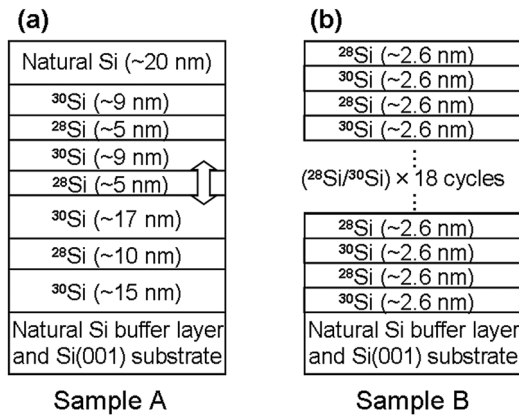


FIG. 1. Structure of the  $^{28}\text{Si}/^{30}\text{Si}$  silicon-isotope multiple layer samples grown by MBE for (a) SIMS measurements (sample A) and (b) AP analysis (sample B). The arrow in (a) indicates the region where the depth resolution parameters were estimated. Sample B in (b) consists of 18 sets of  $^{28}\text{Si}$  ( $\sim 2.6$  nm)/ $^{30}\text{Si}$  ( $\sim 2.6$  nm) layers.

sample A. These depth profiles ( $^{28}\text{Si}$ ,  $^{29}\text{Si}$ , and  $^{30}\text{Si}$ ) were prepared from the columnar volume ( $\varnothing 25$  nm  $\times$  100 nm depth) obtained from the three-dimensional AP analysis data. The procedures for AP analysis are described in detail later. The depth profile of  $^{28}\text{Si}$  was used as the original depth profile of sample A for evaluation of the SIMS depth resolution described hereafter because AP analysis has been reported to provide a higher depth resolution than SIMS even when a low-energy primary ion is used for SIMS measurements.<sup>14,15</sup> The AP depth profile in Fig. 2 shows a significant spread of the  $^{28}\text{Si}$  and  $^{30}\text{Si}$  profiles toward the surface with exponential growth at the  $^{30}\text{Si}/^{28}\text{Si}$  and the  $^{28}\text{Si}/^{30}\text{Si}$  interfaces. This spread is thought to be caused by residual silicon gas elements in the vacuum chamber during MBE growth.

SIMS measurements of sample A were performed under the conditions described in Table I using oxygen ions ( $\text{O}_2^+$ ) and cesium ions ( $\text{Cs}^+$ ) with SIMS 4550 (Cameca) and SIMS

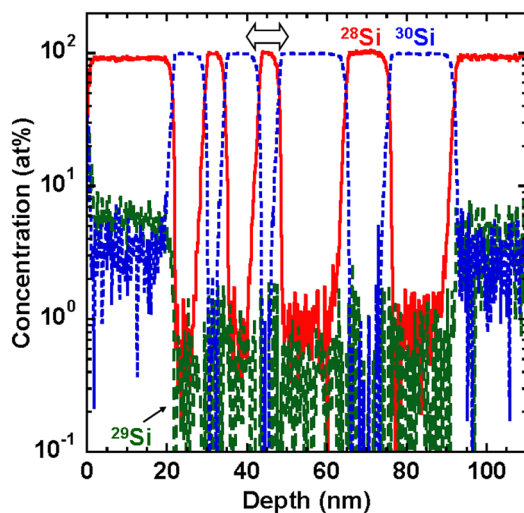


FIG. 2. (Color online) Silicon isotope depth profiles for sample A ( $^{28}\text{Si}$ ,  $^{29}\text{Si}$ , and  $^{30}\text{Si}$ ) measured by AP analysis ( $^{28}\text{Si}$ : solid line,  $^{29}\text{Si}$ : dashed line, and  $^{30}\text{Si}$ : dotted line). The  $^{28}\text{Si}$  depth profile indicated by the arrow was used as the original depth profile for evaluation of the SIMS depth resolution function.

4000 (Cameca) instruments. SIMS 4000, an older instrument, was used for 10 keV  $\text{O}_2^+$  ion bombardments, because SIMS 4550 cannot emit ion beams with energies greater than 5 keV. The  $^{28}\text{Si}^+$ ,  $^{29}\text{Si}^+$ , and  $^{30}\text{Si}^+$  secondary ions produced by  $\text{O}_2^+$  ion bombardment and the  $^{28}\text{Si}^-$ ,  $^{29}\text{Si}^-$ , and  $^{30}\text{Si}^-$  secondary ions produced by  $\text{Cs}^+$  ion bombardment were mass-analyzed/detected with the quadrupole mass analyzer of the SIMS instruments. The depth resolution parameters (the decay length and the standard deviation) were estimated from the  $^{28}\text{Si}$  depth profiles of the fifth layer from the surface, depth of  $\sim 40$ – $50$  nm. Only SIMS measurement conditions that resulted in no ripple (surface roughness) on the sputtered surface were selected based on the methods used in selected references.<sup>5–8</sup> Sputtered surfaces that are fully oxidized by  $\text{O}_2^+$  ion bombardment are known to be smooth.<sup>6,16</sup> Even if the surface is not fully oxidized there are no ripples on the sputtered surface from the surface to the critical depth for ripple formation; however, low  $\text{O}_2^+$  ion energies lead to small critical depths for ripple formation. Wittmaack has shown that the critical depth for 1 keV  $\text{O}_2^+$  ion bombardment with incident angles of  $55^\circ$ – $62^\circ$ , which is a condition corresponding to the minimum energy that produces a surface that is not fully oxidized in this study, is  $\sim 50$  nm.<sup>5</sup> Therefore, the estimated depth resolution parameters are not affected by ripple formation in this study. Surfaces that were or were not fully oxidized were produced depending on the incident angle and the energy of the  $\text{O}_2^+$  ion beam.<sup>5,6</sup> The  $\text{O}_2^+$  ion bombardment conditions that produced full oxidation are marked by asterisks (\*) in Table I. Under  $\text{Cs}^+$  ion bombardment, ripple formation has been reported for large incident angles; therefore, conditions that did not cause ripples were chosen referring to the study of Kataoka *et al.*<sup>8</sup> The depth scale of the SIMS depth profiles was not calibrated based on the sputter crater depth because the craters were shallow (less than 100 nm in depth), resulting in poor measurement precision of the crater depth by the stylus profilometer. Instead, the sputtering rate calculated from sputtering time and the distance (14.1 nm) between the leading edges of the third and the fifth  $^{28}\text{Si}$  layers from the surface was used for the depth calibration. This depth calibration can avoid the problem of the change of sputtering rate in the transient region.<sup>17</sup>

Aligned HR-RBS measurements of the ion-bombarded Si (001) substrate (sample C) were performed using an HRBS500 instrument (Kobe Steel, Ltd.) to evaluate the

TABLE I. SIMS measurement conditions for sample A using  $\text{O}_2^+$  and  $\text{Cs}^+$  ions with a SIMS4550 or SIMS4000 instrument.<sup>a</sup>

| Incident angle (deg) | Primary ion energy (keV)          |                                   |                                   |                                   |                                   |                   |
|----------------------|-----------------------------------|-----------------------------------|-----------------------------------|-----------------------------------|-----------------------------------|-------------------|
|                      | 0.2                               | 0.5                               | 1                                 | 2                                 | 5                                 | 10                |
| 20                   |                                   |                                   | $\text{Cs}^+$ , $\text{O}_2^{+*}$ | $\text{Cs}^+$ , $\text{O}_2^{+*}$ | $\text{Cs}^+$ , $\text{O}_2^{+*}$ | $\text{O}_2^{+*}$ |
| 30                   |                                   | $\text{Cs}^+$ , $\text{O}_2^{+*}$ |                                   |                                   |                                   |                   |
| 40                   | $\text{Cs}^+$ , $\text{O}_2^{+*}$ |                                   |                                   |                                   |                                   |                   |
| 50                   |                                   | $\text{Cs}^+$                     |                                   |                                   |                                   |                   |
| 60                   |                                   |                                   | $\text{Cs}^+$ , $\text{O}_2^+$    | $\text{Cs}^+$ , $\text{O}_2^+$    | $\text{Cs}^+$ , $\text{O}_2^+$    | $\text{O}_2^+$    |

<sup>a</sup>An asterisk (\*) indicates that full oxidation was achieved by the  $\text{O}_2^+$  ions.

TABLE II. Ion sputtering conditions for the Si (001) substrate (sample C) using  $O_2^+$  and  $Cs^+$  ions with a SIMS4550 or SIMS4000 instrument before aligned HR-RBS measurements.

| Incident angle (deg) | Primary ion energy (keV) |               |               |         |
|----------------------|--------------------------|---------------|---------------|---------|
|                      | 1                        | 2             | 5             | 10      |
| 20                   | $Cs^+, O_2^+$            | $Cs^+, O_2^+$ | $Cs^+, O_2^+$ | $O_2^+$ |
| 60                   | $Cs^+, O_2^+$            | $Cs^+, O_2^+$ | $Cs^+, O_2^+$ | $O_2^+$ |

damage depth of the surface. Before the aligned HR-RBS measurements, the sample C surface (area:  $>2\text{ mm} \times 2\text{ mm}$ ) was sputtered with  $O_2^+$  or  $Cs^+$  ion (bombardment conditions: as listed in Table II) using a SIMS 4550 or SIMS 4000 instrument until the sputter equilibrium<sup>18</sup> was reached, i.e., until the silicon secondary ion signal was stable. In the aligned HR-RBS measurements the sample C surface, which was pre-sputtered with  $Cs^+/O_2^+$  ions, was bombarded with 450 keV  $He^+$  ions at an incident angle of  $45^\circ$  relative to the surface normal along the [101] channel of the silicon crystal. The  $He^+$  ions that scattered from the surface with a scatter angle of  $65^\circ$  were energy-analyzed with a sector magnetic spectrometer and were detected by a one-dimensional position-sensitive detector.

AP analysis of the ion-bombarded/sputtered  $^{28}Si/^{30}Si$  isotope multiple layer samples (sample B) was performed with a LEAP3000XSi instrument (Cameca) to evaluate the mixing depth and the degree of mixing of the ion-bombarded sample B surface. Before AP analysis the sample B surface (area:  $\sim 200\ \mu\text{m} \times \sim 200\ \mu\text{m}$ ) was sputtered with  $O_2^+$  or  $Cs^+$  ion using a SIMS 4550 or SIMS 4000 instrument. The sputter depth was  $\sim 22\text{ nm}$  (eight or nine Si isotope layers), which was greater than the equilibrium depth<sup>18</sup> of the surface concentration of the primary ion species under the conditions in the Table III. A nickel protection layer with a thickness of  $\sim 150\text{ nm}$  was deposited with a conventional sputter coater on the  $O_2^+/Cs^+$  ion-bombarded sample B surface, and sample B was then processed into a needle using a focused ion beam instrument with a focused Ga ion beam. The needle was formed in the direction parallel to the depth direction of sample B because the atom probe has a high spatial resolution in the direction of the needle.<sup>15</sup> A green laser with a wavelength of 532 nm and a pulse energy of 0.3 nJ was employed for the AP analysis, and the needle-shaped sample was cooled to a base temperature of  $\sim 30\text{ K}$ . The 3D atom mapping data obtained from the measurements were reconstructed based on the depth scale information from the SIMS data. The initial surface before deposition of the nickel protection layer was determined to be the position where the nickel concentration fell to 50%. The depth profiles were

TABLE III. Ion sputtering conditions for sample B using  $O_2^+$  and  $Cs^+$  ions with a SIMS4550 or SIMS4000 instrument before AP analysis.

| Incident angle (deg) | Primary ion energy (keV) |               |               |         |
|----------------------|--------------------------|---------------|---------------|---------|
|                      | 1                        | 2             | 5             | 10      |
| 60                   | $Cs^+, O_2^+$            | $Cs^+, O_2^+$ | $Cs^+, O_2^+$ | $O_2^+$ |

prepared from the columnar volume ( $\varnothing 10\text{--}25\text{ nm} \times 100\text{ nm}$  depth) in the reconstructed 3D atom data. Figure 3 shows the silicon isotope ( $^{28}Si$  and  $^{30}Si$ ) depth profiles of the original sample B (not bombarded with  $O_2^+/Cs^+$  ions) measured by AP analysis. The 18 sets of  $^{28}Si$  and  $^{30}Si$  layers with layer thicknesses of  $\sim 2.6\text{ nm}$  can be observed separately.

### III. RESULTS AND DISCUSSION

#### A. SIMS depth resolution function

Typical SIMS depth profiles for sample A measured with  $O_2^+$  and  $Cs^+$  ions ( $O_2^+$ : 200 eV,  $40^\circ$ ,  $Cs^+$ : 200 eV,  $40^\circ$ ) are shown in Figs. 4(a) and 4(b), respectively. The SIMS depth resolution parameters were estimated from the  $^{28}Si$  depth profiles of the fifth layer from the surface. The depth profile for  $^{28}Si$  ions measured with  $Cs^+$  ions with low count rates in Fig. 4(b) shows significant edge effects;<sup>18</sup> therefore, in this case, only the high-intensity region [from 42 to 50 nm in Fig. 4(b)] of the depth profile for  $^{28}Si$  ions was used for extraction of the depth resolution parameters.

For evaluation of the depth resolution parameters a convolution calculation was performed with the original depth profile measured using AP analysis (shown in Fig. 2) and the depth resolution function for SIMS analysis. Dowsett *et al.* have indicated that the depth resolution function is a convolution of the exponential growth function, the exponential decay function, and the Gaussian function.<sup>2</sup> However, Chu and Dowsett have shown that for boron delta-doped samples deposited by MBE, the growth length for the exponential growth function in the depth resolution function for boron in a silicon matrix is close to 0 nm.<sup>3</sup> Tomita *et al.* have confirmed the same for boron delta-doped samples fabricated by electron beam deposition near room temperature.<sup>19</sup> Based on the findings of these previous studies, the depth resolution function for use in this study was composed of a convolution of two functions, the exponential decay function and the

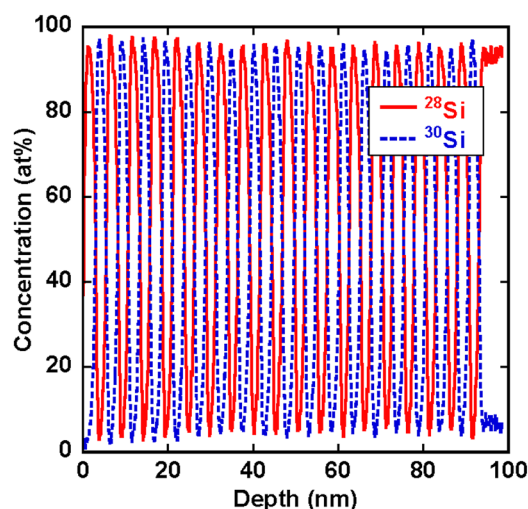


FIG. 3. (Color online) Silicon isotope ( $^{28}Si$  and  $^{30}Si$ ) depth profiles of the original (without ion bombardment) sample B measured by AP analysis ( $^{28}Si$ : solid line and  $^{30}Si$ : dotted line). Each of the  $^{28}Si$  and  $^{30}Si$  layers can be observed separately. Sample B consists of 18 sets of  $^{28}Si$  ( $\sim 2.6\text{ nm}$ )/ $^{30}Si$  ( $\sim 2.6\text{ nm}$ ) layers.

Gaussian function, with the two parameters being the decay length and the standard deviation. This depth resolution function can be expressed as

$$R(z) = A(1 + \operatorname{erf}\xi) \exp\left[-z/\lambda_d + 0.5(\sigma/\lambda_d)^2\right], \quad (1)$$

where  $\xi$  is  $(z/\sigma - \sigma/\lambda_d)/\sqrt{2}$ ,  $\lambda_d$  is the decay length,  $\sigma$  is the standard deviation, and  $A$  is a constant used to normalize integration of the equation. Figure 5 shows the depth profile of  $^{28}\text{Si}$  (SIMS), the original depth profile of  $^{28}\text{Si}$  (obtained by AP analysis), and the convoluted depth profile with the original depth profile and the depth resolution function indicated in Eq. (1) with  $\lambda_d$  and  $\sigma$  optimized to extract these values around the fifth layer of sample A. The optimization of  $\lambda_d$  and  $\sigma$  was performed visually by identifying where the convoluted depth profile coincided most with the SIMS depth profile in the high-intensity region. The SIMS depth profile in Fig. 5 was measured with  $\text{O}_2^+$  ions (200 eV,  $40^\circ$ ), which provided the sharpest depth resolution function in this study. The three depth profiles at the leading edge of the fifth

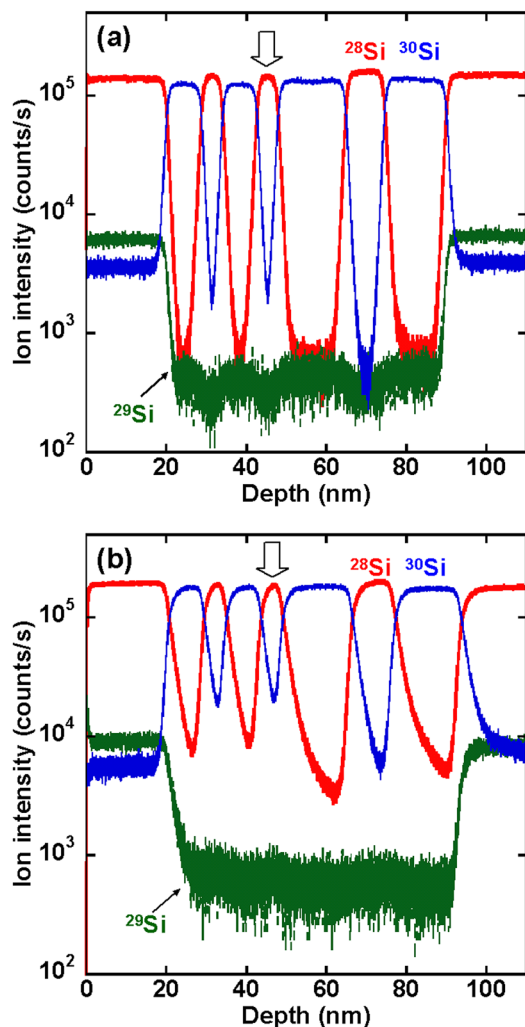


FIG. 4. (Color online) Typical SIMS depth profiles for sample A measured with (a)  $\text{O}_2^+$  ions (200 eV,  $40^\circ$ ) and (b)  $\text{Cs}^+$  ions (200 eV,  $40^\circ$ ). The depth resolution parameters for SIMS analysis were estimated from the  $^{28}\text{Si}$  depth profiles for the fifth layer from the surface (indicated by arrows).

layer agree well, suggesting that the SIMS depth resolution function of silicon in a silicon matrix does not need the exponential growth function component.

The extracted depth resolution parameters under  $\text{O}_2^+$  ion bombardment (with and without full oxidation) and  $\text{Cs}^+$  ion bombardment are plotted against  $E^{1/2}\cos\theta$  ( $E$ : primary ion energy per atom (e.g., 1 keV for a 2 keV  $\text{O}_2^+$  ion beam),  $\theta$ : incident angle relative to the surface normal) in Figs. 6(a) and 6(b), respectively, referring to the relationship proposed by Linnarsson and Svensson.<sup>4</sup> Both parameters, namely the decay length and the standard deviation, can clearly be seen to have linear relationships with  $E^{1/2}\cos\theta$ .

Under  $\text{Cs}^+$  ion bombardment, all the extracted decay lengths and standard deviations are on their corresponding lines despite the wide range of  $\text{Cs}^+$  ion beam incident angles used ( $20^\circ$ – $60^\circ$ ). The depth resolution parameters under  $\text{O}_2^+$  ion bombardment without full oxidation (incident angle of  $60^\circ$ ) are different from those under  $\text{O}_2^+$  ion bombardment with full oxidation (incident angles of  $20^\circ$ ,  $30^\circ$ , or  $40^\circ$ ). Note that the depth resolution parameters under  $\text{O}_2^+$  ion bombardment with full oxidation also show linear relationships with  $E^{1/2}$  because of the relatively small effect of the incident angle.<sup>7</sup>

The depth resolution parameters plotted against  $E^{1/2}\cos\theta$  are smaller for  $\text{O}_2^+$  ion bombardment with full oxidation because of the buffer effect resulting from matrix swelling in the altered layer.<sup>9,20–23</sup> Here,  $\text{O}_2^+$  ion bombardment under conditions where the sputter yield is low creates  $\text{SiO}_2$ , which occupies 2.12 times the volume of silicon (2.12 is the ratio of the silicon atom density in a silicon crystal to that in  $\text{SiO}_2$ ).<sup>23</sup> The atomic mixing takes place in a swollen matrix and the depth resolution parameters therefore become small. The depth resolution parameters, when the surface is not fully oxidized, are 2.12 times those when the surface is fully oxidized as can be seen from the plots against  $E^{1/2}\cos\theta$  in Figs. 7(a) and 7(b).

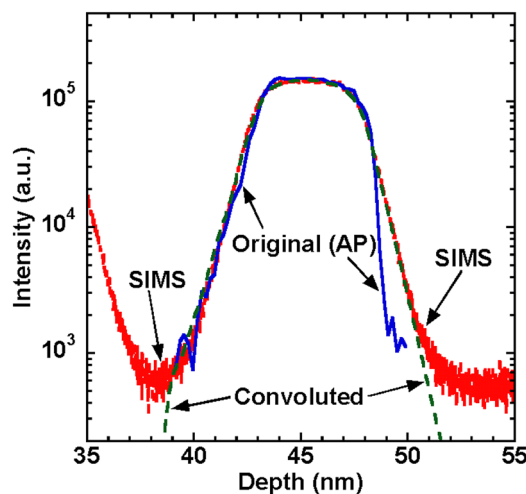


FIG. 5. (Color online) Depth profile for  $^{28}\text{Si}$  (SIMS), the original depth profile for  $^{28}\text{Si}$  (AP analysis), and convoluted depth profile with the original depth profile and depth resolution function indicated in Eq. (1), where  $\lambda_d$  and  $\sigma$  were optimized to extract these values around the fifth layer in sample A. The SIMS depth profile was measured with  $\text{O}_2^+$  ions (200 eV,  $40^\circ$ ).

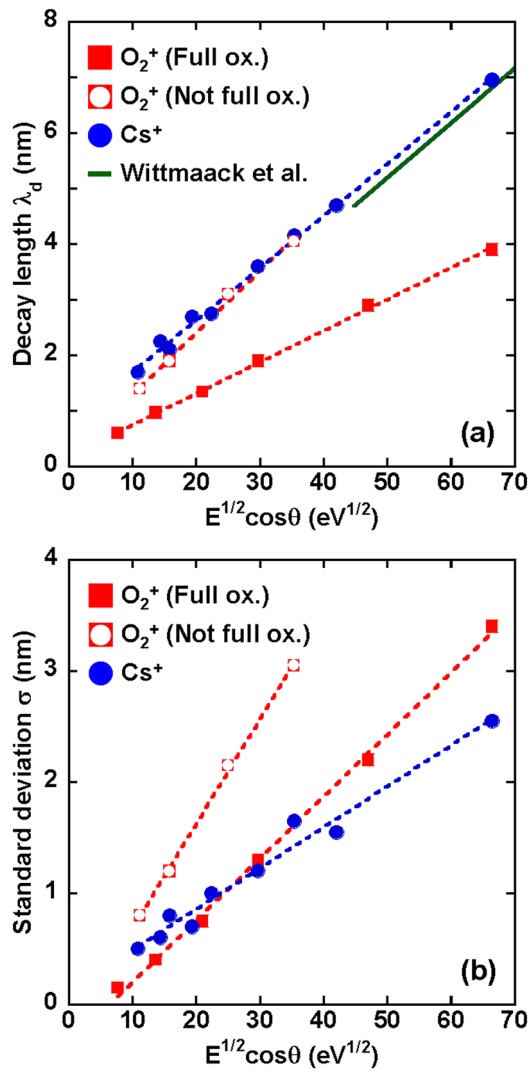


FIG. 6. (Color online) Extracted depth resolution parameters plotted against  $E^{1/2} \cos \theta$  ( $E$ : primary ion energy per atom,  $\theta$ : incident angle relative to the surface normal): (a) decay length and (b) standard deviation for  $O_2^+$  ion bombardment with full oxidation (■),  $O_2^+$  ion bombardment without full oxidation (□), and  $Cs^+$  ion bombardment (●). The solid line in (b) indicates the decay length reported by Wittmaack *et al.* (Ref. 9) for noble gas and Cs ion bombardments.

It is also interesting to compare the depth resolution parameters under  $Cs^+$  ion bombardment with those under  $O_2^+$  ion bombardment without full oxidation in Figs. 6(a) and 6(b). These decay lengths are almost the same at the same  $E^{1/2} \cos \theta$ , thus, there is no mass dependence in these relationships. This result agrees with the studies of Linnarsson and Svensson<sup>4</sup> and Wittmaack and Poker.<sup>9</sup> In addition, the obtained decay lengths are consistent with the results of Wittmaack and Poker, measured under noble gas and  $Cs^+$  ion bombardments [plotted in Fig. 6(a)].<sup>9</sup> On the other hand, the relationships for the standard deviations are different under  $Cs^+$  ion and  $O_2^+$  ion bombardments. The standard deviation for  $O_2^+$  (lighter mass) ion bombardment is greater than that for  $Cs^+$  (heavier mass) ion bombardment, which is also consistent with the studies of Linnarsson and Svensson<sup>4</sup> and Wittmaack and Poker.<sup>9</sup> Even the standard deviations for

$O_2^+$  ion bombardment with full oxidation are greater than those for  $Cs^+$  ion bombardment in the high  $E^{1/2} \cos \theta$  range.

## B. Damage depth measured using aligned HR-RBS

In order to understand the physical meanings of the relationships between the depth resolution parameters and  $E^{1/2} \cos \theta$ , the damage depth of sample C [Si (001) substrate] sputtered by  $O_2^+/Cs^+$  ions under various conditions (listed in Table II) was measured using aligned HR-RBS. The damage depth corresponds to the short-range displacement of silicon atoms from the periodic position in the silicon crystal during atomic mixing by ion bombardment. Figure 8 shows typical aligned HR-RBS spectra for sample C bombarded by  $O_2^+$  ions [10 keV, 60° (5 keV per single O atom)] and  $Cs^+$  ions (5 keV, 60°). A damaged silicon peak, an oxygen peak (under  $Cs^+$  ion bombardment, this peak is probably caused by oxidation of cesium in the air), and a cesium peak (only under  $Cs^+$

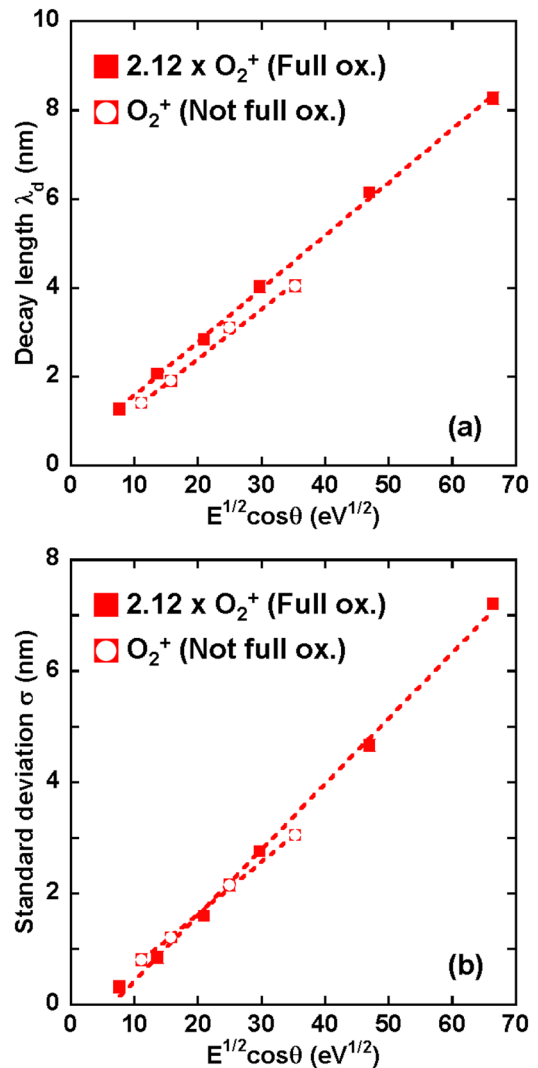


FIG. 7. (Color online) Depth resolution parameters plotted against  $E^{1/2} \cos \theta$  ( $E$ : primary ion energy per atom,  $\theta$ : incident angle relative to the surface normal): (a) decay length and (b) standard deviation for  $O_2^+$  ion bombardment with full oxidation (■), and  $O_2^+$  ion bombardment without full oxidation (□). The depth resolution parameters when the surface is not fully oxidized are 2.12 times those when the surface is fully oxidized.

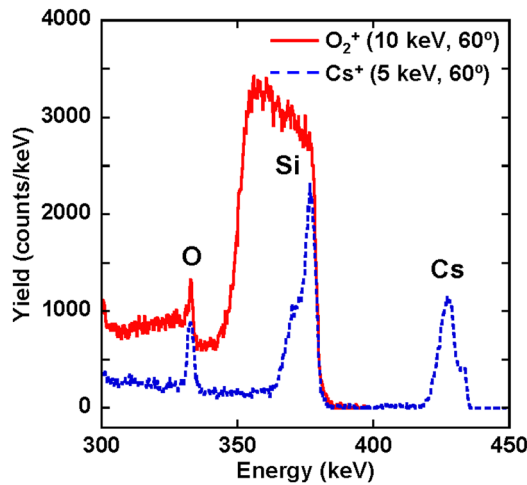


Fig. 8. (Color online) Typical aligned HR-RBS spectra for sample C (Si (001) substrate) bombarded by  $O_2^+$  ions [10 keV,  $60^\circ$  (5 keV per single O atom)] and  $Cs^+$  ions (5 keV,  $60^\circ$ ).

ion bombardment) can be seen. Although the bombardment conditions have almost the same decay length (4.1 nm for  $O_2^+$  ions and 4.2 nm for  $Cs^+$  ions), the total amounts of signals from the damaged silicon peak are quite different. The aligned HR-RBS results also indicated that the  $20^\circ$  incident conditions (not shown here) for the  $O_2^+$  and  $Cs^+$  ions, respectively, provided higher oxygen and cesium concentrations near the sputtered surface than those provided by the corresponding  $60^\circ$  incident conditions because of the reduction in sputtering yield with the increase in angle of incidence.<sup>24</sup>

The relationships of the damage depths for sample C measured using aligned HR-RBS with the SIMS depth resolution parameters under various  $O_2^+$  and  $Cs^+$  ion bombardment conditions are shown in Fig. 9. The damage depths were calculated from the integrated signals for the damaged silicon peaks in the aligned HR-RBS spectra. The silicon signals from thermally grown  $SiO_2$ /silicon crystals (observed

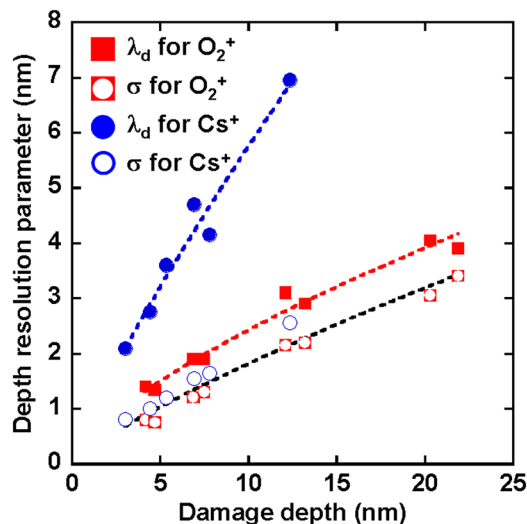


Fig. 9. (Color online) Relationships between the sample C [Si (001) substrate] damage depth (measured by aligned HR-RBS) and the depth resolution parameters (decay length,  $\lambda_d$ , and standard deviation,  $\sigma$ ) for  $O_2^+$  and  $Cs^+$  ion bombardment.

using aligned HR-RBS) have been attributed to Si atoms in  $SiO_2$ . They have also been attributed to (i) the interface peak (surface peak from an ideally terminated silicon crystal surface), (ii) Si atoms in the suboxide state, and (iii) lattice distortion of silicon near the interface.<sup>25,26</sup> In this study, signals from the suboxide at the interface of the  $O_2^+$  ion-bombarded samples should also be regarded as those from damaged silicon. The silicon signal value from the interface peak is assumed to be almost the same as that reported,<sup>25</sup> but there is no information on the signals from lattice distortion near the interface between the ion-bombarded (damaged) layer and the silicon crystal. In this study it was assumed that signals from damaged silicon could be obtained by subtracting the interface peak signal ( $2.67 \times 10^{15}$  atoms/cm<sup>2</sup> in Ref. 25) from the integrated silicon signals. This assumption is not expected to affect the results significantly because the contribution of silicon signals from the lattice distortion to the integrated silicon signal is relatively small as the silicon signal from the lattice distortion in an  $SiO_2$ /Si system is less than  $1.7 \times 10^{15}$  atoms/cm<sup>2</sup> in Ref. 25, whereas the minimum silicon signal from damaged silicon in this study was  $1.5 \times 10^{16}$  atoms/cm<sup>2</sup>. The damage depths were calculated from the signals from the damaged silicon (unit: atoms/cm<sup>2</sup>) and the silicon atomic density ( $5.0 \times 10^{22}$  atoms/cm<sup>3</sup>).<sup>27</sup> It should be noted that the damage depths calculated here correspond to the initial thickness of silicon crystal damaged by ion bombardment, and not to the thickness after the matrix swelling due to the incorporation of O/Cs.

The relationships in Fig. 9 show interesting results. The plots of the standard deviation versus damage depth depend only on the damage depth. There is a small dependence on the ion species ( $O_2^+$ / $Cs^+$ ) and none on the different sputtered surface conditions caused by the different incident angles, namely, fully oxidized/not fully oxidized in the case of  $O_2^+$  ion bombardment or differing surface cesium content in the case of  $Cs^+$  ion bombardment. On the other hand, the plots of the decay length versus the damage depth depend on both the damage depth and the ion species, but not on the sputtered surface condition. Thus, the relationships for  $O_2^+$  ion and  $Cs^+$  ion bombardments differ from each other. These results suggest that the damage depth is a determining factor for the standard deviation. Therefore, the standard deviation is greater for ion bombardment with a lighter mass (greater penetration depth) under the same bombardment conditions as already reported.<sup>4,9</sup> The decay length; however, depends not only on the damage depth, but also on factors that have not yet been clarified.

### C. Mixing depth and degree of mixing measured by AP analysis

To investigate the atomic mixing effect of the  $O_2^+$  and  $Cs^+$  ion bombardments, AP analysis was performed. Figures 10(a) and 10(b), respectively, show the AP depth profiles of the sample B surfaces that were bombarded by  $O_2^+$  ions (2 keV,  $60^\circ$ ) and  $Cs^+$  ions (5 keV,  $60^\circ$ ) until the sputter equilibrium was reached. The thin lines in Figs. 10(a) and 10(b) are the depth profiles of the original (nonbombarded) sample B,

which have already been shown in Fig. 3. These AP depth profiles directly indicate how  $O_2^+/Cs^+$  ions produce atomic mixing near the sputtered sample B surface. Large differences between the depth profiles in Figs. 10(a) and 10(b) can be seen near the sputtered surface. Both the  $O_2^+$  and  $Cs^+$  ion bombarded surfaces show significant atomic mixing relative to the original sample. The atomic mixing between the  $^{28}Si$  and  $^{30}Si$  layers is greater for the  $Cs^+$  ion bombarded surface than for the  $O_2^+$  ion bombarded surface even though the damage depths measured for the two surfaces using aligned HR-RBS are similar; 6.9 nm for  $O_2^+$  ion bombardment and 7.8 nm for  $Cs^+$  ion bombardment. Here we define two parameters to quantify the atomic mixing between the  $^{28}Si$  and  $^{30}Si$  layers. The first is the mixing depth, which is defined as the depth from the sample surface where the original and bombarded profiles coincide. The mixing depth indicates long-range atomic mixing by the exchange of silicon isotope atoms between isotope layers in both the depth and surface directions. These AP depth profiles are not precise

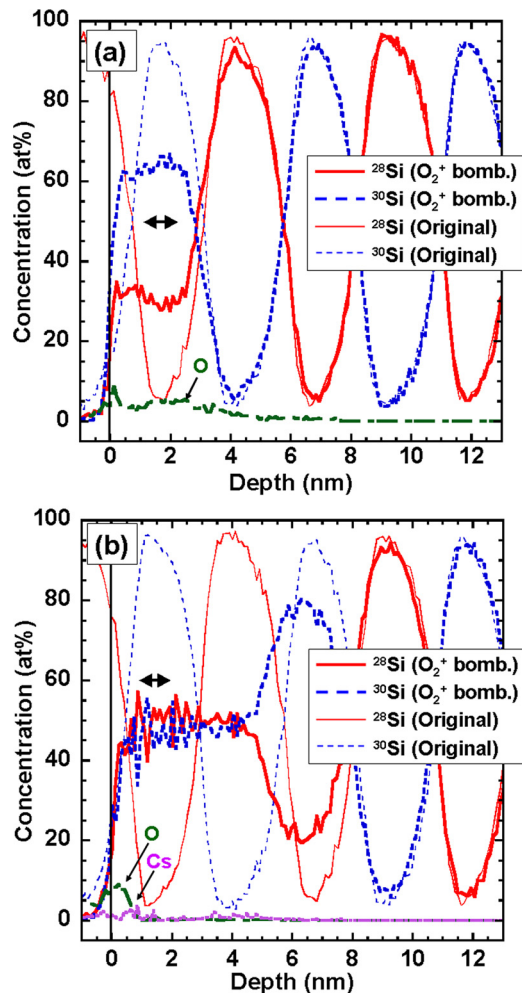


FIG. 10. (Color online) AP depth profiles for sample B surfaces bombarded by (a)  $O_2^+$  ions (2 keV,  $60^\circ$ ) and (b)  $Cs^+$  ions (5 keV,  $60^\circ$ ) until the sputter equilibrium was reached ( $^{28}Si$ : thick solid line,  $^{30}Si$ : thick dotted line). The thin lines are the depth profiles of the original (nonbombarded) sample B ( $^{28}Si$ : thin solid line,  $^{30}Si$ : thin dotted line). The surface (0 nm) of the bombarded sample B was determined to be the position where the nickel concentration fell to 50%. The arrows indicate the antinode region of the wave-like depth profiles for calculation of the degree of mixing (DM).

because of the limited signal intensity and; therefore, there is some uncertainty ( $\sim 1$  nm or less) in the obtained mixing depths. The second parameter for quantifying the atomic mixing is the degree of mixing (DM) near the sputtered surface, which can be expressed as

$$DM = 1 - \frac{|C_{^{28}Si} - C_{^{30}Si}|}{(C_{^{28}Si} + C_{^{30}Si})}, \quad (2)$$

where  $C_{^{28}Si}$  and  $C_{^{30}Si}$  are, respectively, the concentrations of  $^{28}Si$  and  $^{30}Si$  near the sputtered surface. The  $C_{^{28}Si}$  and  $C_{^{30}Si}$  values used for the calculation were obtained from the antinode region ( $\sim 1$  nm width) near the sputtered surface (from  $\sim 1$  to  $\sim 3$  nm depth) of the wave-like depth profiles in Figs. 10(a) and 10(b). When the  $^{28}Si$  and  $^{30}Si$  layers are perfectly mixed DM becomes 1, and when they are perfectly separated DM becomes 0. Note that the calculated degree of mixing is affected not only by atomic mixing, but also by the endpoint of ion sputtering. However, as the isotopic silicon layers ( $^{28}Si$  and  $^{30}Si$  layers) are thin (2.6 nm), the influence of the ion-sputtering endpoint on the degree of mixing is limited. We; therefore, think that the degree of mixing reveals the atomic mixing status near the sputtered surface. When the degree of mixing becomes high, the depth resolution of the SIMS depth profile is thought to deteriorate. In other words, the values of the depth resolution parameters, namely the decay length and/or the standard deviation, are thought to increase.

The relationship between the damage depth measured using aligned HR-RBS and the mixing depth measured using AP analysis under  $O_2^+$  and  $Cs^+$  ion bombardment is plotted in Fig. 11(a). Only one curve can be seen in Fig. 11 because the relationship is independent of the ion species ( $O_2^+/Cs^+$ ). The slope of the curve is  $\sim 1$  up to a depth of  $\sim 12$  nm, indicating that defect formation induced by the ion bombardment results in atomic mixing between the silicon isotopic layers. Beyond  $\sim 12$  nm the mixing depth is greater than the damage depth. This may be due to partial damage, i.e., a mixture of damaged silicon and crystalline silicon, in deep regions. On the other hand, the relationship between the damage depth and the degree of mixing depends on the ion species ( $O_2^+/Cs^+$ ), as can be seen in Fig. 11(b). This figure reveals that at the same damage depth, i.e., at the same standard deviation, the degree of mixing differs for  $O_2^+$  and  $Cs^+$  ion bombardments. This may be due to larger elastic recoil implantation for  $Cs^+$  ion bombardment, because the higher nuclear charge of the primary ion may produce a larger elastic recoil implantation yield,<sup>28</sup> and greater atomic mixing following recoil implantation. Figure 12 shows the relationships between the degree of mixing and the depth resolution parameters. This figure indicates that the decay length is degraded according to the degree of mixing without any dependence on the ion species ( $O_2^+/Cs^+$ ).

## D. Atomic mixing/sputtering simulations

Atomic mixing/sputtering simulations were performed in order to investigate the physical meanings of the decay

length degradation and the relationships between the damage depth and the SIMS depth resolution parameters shown in Fig. 9. The simulations were performed referring to the work of Linnarsson and Svensson,<sup>4</sup> who studied the broadening of the SIMS depth profile using a diffusion model for atomic mixing. The model includes surface movement by ion sputtering and variation of the diffusion coefficient with depth. We simulated SIMS depth profiles using their diffusion model for atomic mixing, assuming that diffusion of atoms occurs within regions of dilute concentration even though large numbers of  $^{28}\text{Si}$  and  $^{30}\text{Si}$  atoms actually diffuse between isotope layers. In the diffusion model, each atomic layer is broadened by a Gaussian function with variance,  $v$ , which can be expressed by

$$v = 4Dt = 2/3NR^2, \quad (3)$$

where  $D$  is the diffusion coefficient,  $t$  is the time for diffusion by atomic mixing,  $N$  is the average number of atom displacements by atomic mixing before sputtering, and  $R$  is the step length of atom jumping in the diffusion process.<sup>4</sup> From

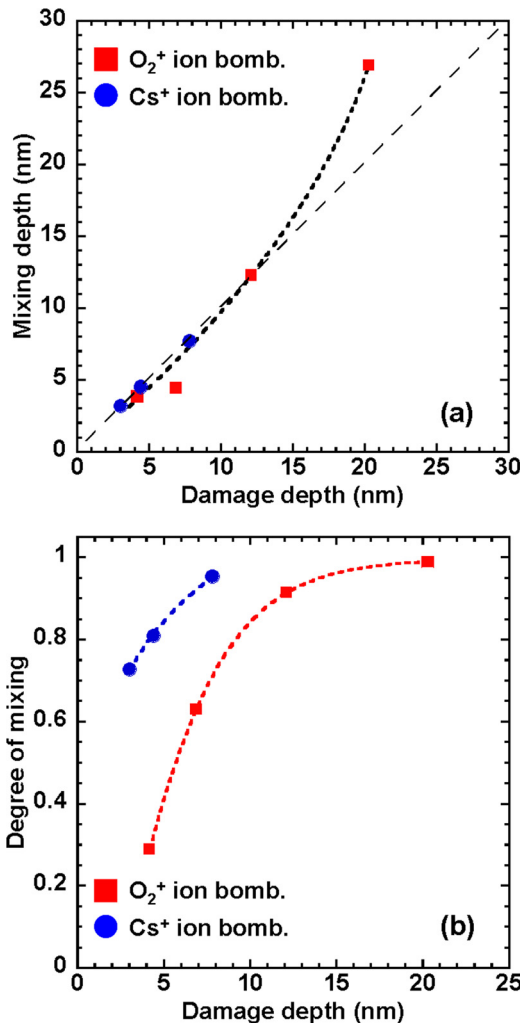


Fig. 11. (Color online) Relationships between the damage depth (measured by aligned HR-RBS) and (a) the mixing depth and (b) the degree of mixing (both measured by AP analysis) for  $\text{O}_2^+$  ion bombardment (■) and  $\text{Cs}^+$  ion bombardment (●).

Eq. (3), if the step length,  $R$ , is assumed to be constant, a large variance [diffusion (atomic mixing) over a long distance] is seen when the number of atom displacements,  $N$ , is large or the sputtering yield is small (the diffusion time,  $t$ , is long). We therefore refer to the variance,  $v$ , as the “damage density” in this study.

Using the diffusion model, SIMS depth profiles for delta-doped layers (i.e., the SIMS depth resolution function) were simulated. Four damage density profiles with different damage densities and depths were used for the simulations. These profiles are shown in Fig. 13(a). Of course, the actual damage density profiles are not box-shaped, as in Fig. 13(a), and should resemble Gaussian functions as predicted by SRIM.<sup>29</sup> But, here the box-shaped damage density profiles are used to obtain simplified relationships between the depth resolution functions and the damage depth and damage density. Figure 13(b) shows simulated SIMS depth resolution functions under ion bombardment conditions corresponding to the damage density profiles shown in Fig. 13(a). The depth profiles in Figs. 13(a) and 13(b) indicate that the standard deviation,  $\sigma$ , which represents Gaussian blurring of the SIMS depth resolution function, mainly depends on the damage depth of the damage density profiles, which agrees with Fig. 9, and indicates that the standard deviation depends on the damage depth and the decay length,  $\lambda_d$ , which represents the length over which the signal of the SIMS depth resolution function attenuates to  $1/e$ , mainly depends on the damage density in the damage density profiles. However, the depth resolution function of Eq. (1) does not provide a good fit for the simulated SIMS resolution functions probably because of the use of box-shaped damage density profiles.

It is thought that the damage density profile has some correlation with the degree of mixing near the sputtered surface. Although the atomic mixing/sputtering simulations in this study can be applied correctly only in regions with dilute concentrations, they provide semiquantitative results for the

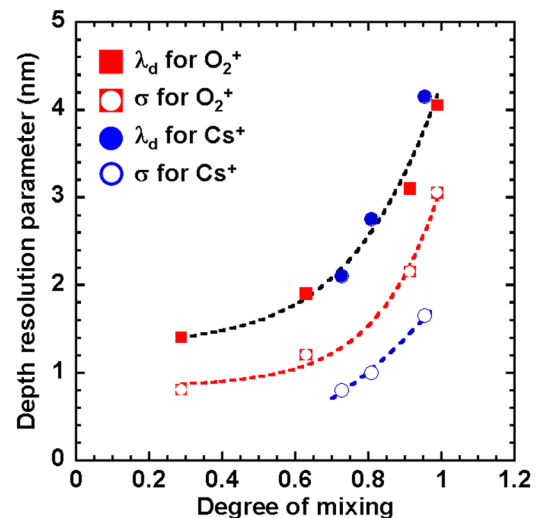


Fig. 12. (Color online) Relationships between the degree of mixing (measured by AP analysis) and the depth resolution parameters (decay length,  $\lambda_d$ , and standard deviation,  $\sigma$ ) for  $\text{O}_2^+$  ion bombardment and  $\text{Cs}^+$  ion bombardment [ $\lambda_d$  for  $\text{O}_2^+$  (■),  $\sigma$  for  $\text{O}_2^+$  (□),  $\lambda_d$  for  $\text{Cs}^+$  (●), and  $\sigma$  for  $\text{Cs}^+$  (○)].

ion-bombarded surface of multiple layer samples. Atomic mixing phenomena near the sputtered surface of multiple layer samples (consisting of alternate layers of layer A and layer B) were calculated by simulation using three damage density profiles with the same damage depth of 8 nm and different damage densities [0.5, 1 (condition A in Fig. 13(a)), and 2 [condition B in Fig. 13(a)]. The original depth profiles of the multiple layers before ion bombardment were set as sine wave functions with a wavelength of 5.2 nm (thickness of layer A = thickness of layer B = 2.6 nm). Figure 14 shows the simulated depth profiles of the ion-bombarded multiple layers (layer A). These results indicate that, for the same damage depth condition, larger damage densities lead to greater atomic mixing near the sputtered surface. From these simulation results and the experimental results shown in Figs. 11(b) and 12 (different degrees of mixing for  $O_2^+$  and  $Cs^+$  ion bombardment at the same damage depth and dependence of the decay length on the degree of mixing), the decay length is thought to depend strongly on the degree of mixing and the damage density. Also,  $Cs^+$  ion bombardment

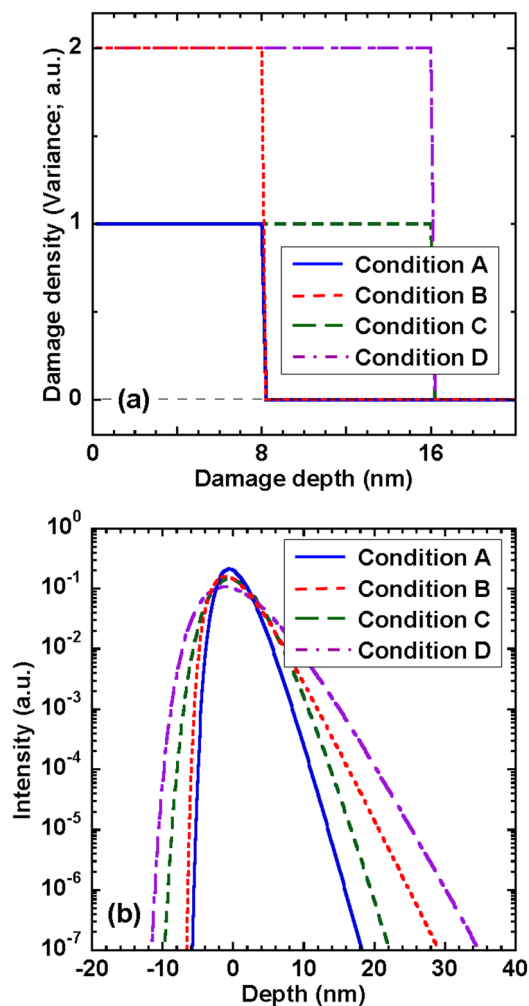


FIG. 13. (Color online) (a) Four damage density profiles with different damage densities and damage depths, used for simulation of atomic mixing/sputtering. (b) Simulated SIMS depth resolution functions under the ion bombardment conditions corresponding to the damage density profiles in (a).

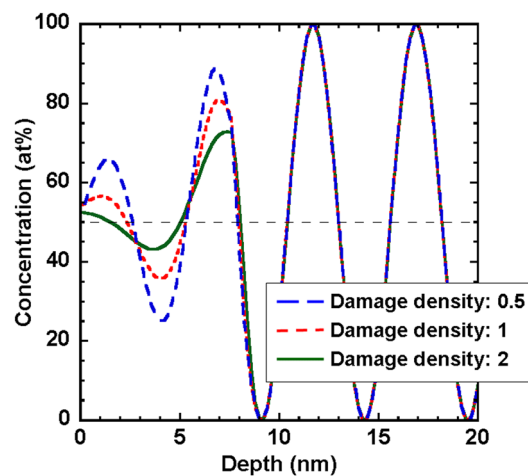


FIG. 14. (Color online) Simulated depth profiles for ion-bombarded multiple layers (layer A; originally set as a sine wave function with a wavelength of 5.2 nm) at the same damage depth of 8 nm for 3 damage density profiles (damage densities of 0.5, 1, and 2).

is thought to lead to larger damage densities; as a result of larger elastic recoil implantation, than  $O_2^+$  ion bombardment for the same damage depth condition, resulting in a longer decay length for  $Cs^+$  ion bombardment at the same damage depth (shown in Fig. 9).

### E. Factors determining the depth resolution parameters

Here, the factors determining the depth resolution parameters, namely, the decay length,  $\lambda_d$ , and the standard deviation,  $\sigma$ , are discussed using the results described previously.

As can be seen in Figs. 9 and 13(b), the standard deviation, which represents Gaussian blurring of the SIMS depth resolution function, is directly correlated with the damage depth. The relationship of the standard deviation versus the damage depth has only a small dependence on the ion species and the damage density and no dependence on the sputtered surface conditions. These findings suggest that the standard deviation is degraded by the following mechanism. Primary ion bombardment deposits energy near the surface and causes atomic mixing in both the surface and depth directions with the formation of a damage layer. When the mixing depth and the damage depth are large, atoms in shallow and deep regions are mixed with a high probability, resulting in the migration of atoms in deep regions to shallow regions. The migration of atoms in shallow regions to deep regions also occurs in atomic mixing, but it is always overshadowed by the exponential decay. The depth resolution function, therefore, shows a long tail toward the surface, or, a large standard deviation. When the damage depth is small even though the damage density (the degree of mixing) is large, atoms in deep regions cannot migrate toward shallow regions, and the depth resolution function shows a short tail toward the surface, or, a small standard deviation. Thus, the standard deviation depends mainly on the damage depth, and the relationship of the standard deviation with the damage depth has a small dependence on the ion species and the

damage density. To measure the upslope depth profiles correctly, SIMS measurement conditions with a short standard deviation should be used; e.g., by using low-energy heavy primary ion ( $\text{Cs}^+$  ion) bombardment or low-energy  $\text{O}_2^+$  ion bombardment with full oxidization, because the standard deviation affects the upslope depth profiles.<sup>30</sup>

On the other hand, the decay length, which represents the length over which the signal of the SIMS depth resolution function attenuates to  $1/e$ , has no direct relationship with the damage depth or the mixing depth, but is correlated with the degree of mixing measured using AP analysis (Fig. 12) and the damage density used in the atomic mixing/sputtering simulations [Fig. 13(b)]. Here we consider sputtering by primary ion bombardment through an atomic layer of species M (marker atoms), in which the ion bombardment causes atomic mixing in both the surface and depth directions and sputtering of the instantaneous surface atoms. After sputtering through the layer of M atoms, the region near the sputtered surface is loaded with M atoms, whose distribution depends on the atomic mixing caused by the ion bombardment. The intensity of the sputtered M atoms depends on the instantaneous surface concentration of species M. The shape of the distribution of M atoms near the sample surface is maintained during sputtering but the total number of M atoms remaining at the surface is reduced. The next sputtering removes M atoms at the surface with a lower intensity because of the lower concentration of species M on the instantaneous surface. These sequential phenomena produce an exponential decay of the intensity of species M. When the damage density is large and; thus, the degree of mixing is also large, the M atoms initially located in the atomic layer of species M are exchanged with atoms in adjacent atomic layers with a high probability, resulting in a long tail of the depth resolution function in the depth direction (long decay length). Thus, the decay length is thought to be degraded by a high degree of atomic mixing near the surface caused by a large damage density. The longer decay length for  $\text{Cs}^+$  ion bombardment relative to  $\text{O}_2^+$  ion bombardment under the same damage depth condition is thought to be because of the larger damage density (higher degree of mixing) near the surface. To measure the downslope depth profiles correctly, SIMS measurement conditions corresponding to a short decay length (e.g., low energy  $\text{O}_2^+$  ion bombardment with full oxidization) should be used because the decay length affects the downslope depth profiles.<sup>30</sup>

Finally, the reason why the decay lengths measured for  $\text{Cs}^+$  ion bombardment and  $\text{O}_2^+$  ion bombardment (without full oxidation) are the same at the same  $E^{1/2}\cos\theta$  in Fig. 6(a) is discussed. Similar phenomena showing no dependence of the decay length on primary ion mass have already reported by Wittmaack and Poker<sup>9</sup> and Linnarsson and Svensson.<sup>4</sup> SRIM<sup>29</sup> predicts higher damage density near the surface under bombardment with heavier ions. This does not mean that heavier ions necessarily produce a higher damage density near the surface, because the sputtering yield also affects the damage density in that low sputtering yields produce high damage per unit depth. Sputtering yields have been reported to be higher for heavier ion bombardment (more than 500 eV).<sup>31</sup> In addition, under  $\text{O}_2^+$  ion bombardment, surface

oxidation suppresses the sputtering yield. The sputtering yield for  $\text{Cs}^+$  ion bombardment is therefore expected to be much higher than that for  $\text{O}_2^+$  ion bombardment at the same  $E^{1/2}\cos\theta$ . The same decay length at the same  $E^{1/2}\cos\theta$  in Fig. 6(a) could be caused by cancellation of the high damage density by the high sputtering yield. However, the damage distributions predicted by SRIM and the experimentally obtained sputtering yields used in the atomic mixing/sputtering simulations cannot explain the decay lengths seen in Fig. 6(a). Further research is needed to clarify why the decay lengths are the same.

#### IV. CONCLUSIONS

In order to identify their controlling factors, the SIMS depth resolution parameters of decay length and standard deviation (also referred to as the SIMS depth resolution function) for silicon atoms in a silicon matrix with silicon-isotope multiple layers were investigated under oxygen ( $\text{O}_2^+$ ) and cesium ( $\text{Cs}^+$ ) ion bombardments with a wide ion energy range (from 200 eV to 10 keV) and with several incident angles. The investigation was performed without the chemical segregation effect and also without ripple formation on the sample surface. The obtained depth resolution parameters were proportional to  $E^{1/2}\cos\theta$  ( $E$ : primary ion energy per atom;  $\theta$ : incident angle relative to the surface normal), and the relationships for the decay length and the standard deviation were different for the  $\text{Cs}^+$  ion, the  $\text{O}_2^+$  ion with full oxidization, and the  $\text{O}_2^+$  ion without full oxidization. However, the decay lengths were similar for the  $\text{Cs}^+$  ion and the  $\text{O}_2^+$  ion without full oxidation). The depth resolution parameters are smaller for  $\text{O}_2^+$  ion bombardment with full oxidization because of the buffer effect of the matrix swelling resulting from oxygen incorporation. Comparing the depth resolution parameters under  $\text{Cs}^+$  ion bombardment and  $\text{O}_2^+$  ion bombardment without full oxidation plotted against  $E^{1/2}\cos\theta$ , the decay lengths were almost the same but the standard deviation was greater for  $\text{O}_2^+$  ion bombardment than for  $\text{Cs}^+$  ion bombardment. These results are consistent with those reported in Refs. 4 and 9. Aligned HR-RBS, AP analysis, and mixing/sputtering simulations were performed in order to understand the physical meanings of the relationships between the depth resolution parameters and  $E^{1/2}\cos\theta$ . The standard deviation plotted against the damage depth depended only on the damage depth measured by aligned HR-RBS. There is only a small dependence on the ion species ( $\text{O}_2^+/\text{Cs}^+$ ) and none on the condition of the sputtered surface and whether it was fully oxidized or not fully oxidized by  $\text{O}_2^+$  ion bombardment. This result suggests that a determining factor of the standard deviation is the damage depth. On the other hand, the decay lengths were found to depend not only on the damage depths but also on the ion species. The degree of mixing near the sputtered surface of thin silicon-isotope multiple layers bombarded/damaged by  $\text{O}_2^+/\text{Cs}^+$  ions was measured using AP analysis and the relationships of the degree of mixing with the depth resolution parameters indicated that the decay length was degraded according to the degree of mixing. The atomic mixing/sputtering simulations

indicated the factors determining the SIMS depth resolution parameters. The standard deviation is mainly degraded by the damage depth (this finding agrees with the aligned HR-RBS result), whereas the decay length is mainly extended by the variance (damage density) of the damage density profiles, which is a parameter of the Gaussian function and governs the degree of mixing near the surface.

In conclusion, the standard deviation is thought to be degraded by the following mechanism. When the damage depth and the mixing depth are large, atoms in shallow and deep regions are mixed with a high probability, resulting in the migration of atoms in deep regions to shallow regions. Therefore, the depth resolution function shows a long tail toward the surface, or, a large standard deviation.

Also, the decay length is thought to be extended by the following mechanism. When the damage density is large and; thus, the degree of mixing is also large, atoms in any particular atomic layer are exchanged with those in adjacent atomic layers with a high probability, resulting in a long tail of the depth resolution function in the depth direction, or, a long decay length.

## ACKNOWLEDGMENTS

The authors are grateful to Y. Hori of Toshiba Nanoanalysis Corporation for the SIMS measurements and data analysis, K. Sasakawa and K. Fujikawa of Kobelco Research Institute, Inc. for the aligned HR-RBS measurements and data interpretation, and H. Uchida, M. Kato, and Ms. N. Arai of Toshiba Nanoanalysis Corporation for the AP analysis and data interpretation. The authors also thank J. Koga, A. Shimazaki, and their colleagues at Toshiba Corporation for their insightful suggestions and financial support.

<sup>1</sup>“Front end processes,” *International Technology Roadmap for Semiconductors (ITRS)*, 2009 ed., <http://www.itrs.net/>.

<sup>2</sup>M. G. Dowsett, G. Rowlands, P. N. Allen, and R. D. Barlow, *Surf. Interface Anal.* **21**, 310 (1994).

<sup>3</sup>D. P. Chu and M. G. Dowsett, *Phys. Rev. B* **56**, 15167 (1997).

<sup>4</sup>M. K. Linnarsson and B. G. Svensson, *Phys. Rev. B* **60**, 14302 (1999).

<sup>5</sup>K. Wittmaack, *J. Vac. Sci. Technol. B* **16**, 2776 (1998).

<sup>6</sup>Z. X. Jiang, J. Lerma, D. Sieloff, J. J. Lee, S. Backer, S. Bagchi, and J. Conner, *J. Vac. Sci. Technol. B* **22**, 630 (2004).

<sup>7</sup>T. Sasaki, N. Yoshida, M. Takahashi, and M. Tomita, *Appl. Surf. Sci.* **255**, 1357 (2008).

<sup>8</sup>Y. Kataoka, K. Yamazaki, M. Shigeno, Y. Tada, and K. Wittmaack, *Appl. Surf. Sci.* **203–204**, 43 (2003).

<sup>9</sup>K. Wittmaack and D. B. Paker, *Nucl. Instrum. Methods Phys. Res. B* **47**, 224 (1990).

<sup>10</sup>Y. Shimizu, A. Takano, M. Uematsu, and K. M. Itoh, *Physica B* **401–402**, 597 (2007).

<sup>11</sup>Y. Shimizu, M. Uematsu, K. M. Itoh, A. Takano, K. Sawano, and Y. Shiraki, *Appl. Phys. Express* **1**, 021401 (2008).

<sup>12</sup>T. Kojima, R. Nebashi, K. M. Itoh, and Y. Shiraki, *Appl. Phys. Lett.* **83**, 2318 (2003).

<sup>13</sup>Y. Shimizu and K. M. Itoh, *Thin Solid Films* **508**, 160 (2006).

<sup>14</sup>Y. Shimizu, Y. Kawamura, M. Uematsu, K. M. Itoh, M. Tomita, M. Sasaki, H. Uchida, and M. Takahashi, *J. Appl. Phys.* **106**, 076102 (2009).

<sup>15</sup>Y. Shimizu *et al.*, *J. Appl. Phys.* **109**, 036102 (2011).

<sup>16</sup>K. Elst, W. Vandervorst, and J. Alay, *J. Vac. Sci. Technol. B* **11**, 1968 (1993).

<sup>17</sup>M. Tomita, M. Suzuki, T. Tachibe, S. Kozuka, and A. Murakoshi, *Appl. Surf. Sci.* **203–204**, 377 (2003).

<sup>18</sup>R. G. Wilson, F. A. Stevie, and C. W. Magee, *Secondary Ion Mass Spectrometry, A Practical Handbook for Depth Profiling and Bulk Impurity Analysis* (Wiley, New York, 1989).

<sup>19</sup>M. Tomita, H. Tanaka, M. Koike, S. Takeno, Y. Hori, and M. Takahashi, *J. Vac. Sci. Technol. B* **27**, 1844 (2009).

<sup>20</sup>M. Meuris and W. Vandervorst, *J. Vac. Sci. Technol. A* **9**, 1482 (1991).

<sup>21</sup>R. D. Barlow, M.G. Dowsett, H. S. Fox, R. A. A. Kubiak, and S. M. Newsstead, *Nucl. Instrum. Methods Phys. Res. B* **72**, 442 (1992).

<sup>22</sup>Z. X. Jiang and P. F. A. Alkemade, *J. Vac. Sci. Technol. B* **16**, 1971 (1998).

<sup>23</sup>C. Tian and W. Vandervorst, *J. Vac. Sci. Technol. A* **15**, 452 (1997).

<sup>24</sup>A. E. Morgan, H. A. M. de Grefte, N. Warmoltz, H. W. Werner, and H. J. Tolle, *Appl. Surf. Sci.* **7**, 372 (1981).

<sup>25</sup>K. Nakajima, M. Suzuki, K. Kimura, M. Yamamoto, A. Teramoto, T. Ohmi, and T. Hattori, *Jpn. J. Appl. Phys.* **45**, 2467 (2006).

<sup>26</sup>A. Bongiorno, A. Pasquarello, M. S. Hybertsen, and L. C. Feldman, *Phys. Rev. B* **74**, 075316 (2006).

<sup>27</sup>*Properties of Silicon, EMIS Datareviewers Series No. 4* (INSPEC, The Institute of Electrical Engineers, London, 1988).

<sup>28</sup>O. Kruse and H. D. Carstanjen, *Nucl. Instrum. Methods Phys. Res. B* **89**, 191 (1994).

<sup>29</sup>J. F. Ziegler, “The stopping and range of ions in matter (SRIM-2008),” <http://www.srim.org/>.

<sup>30</sup>M. Tomita, C. Hongo, M. Suzuki, M. Takenaka, and A. Murakoshi, *J. Vac. Sci. Technol. B* **22**, 317 (2004).

<sup>31</sup>P. C. Zalm, *J. Appl. Phys.* **54**, 2660 (1983).